PERGAMON

International Journal of Solids and Structures 40 (2003) 6613–6631

INTERNATIONAL JOURNAL OF SOLIDS and STRUCTURES

www.elsevier.com/locate/ijsolstr

An efficient higher order zigzag theory for composite and sandwich beams subjected to thermal loading

S. Kapuria *, P.C. Dumir, A. Ahmed

Department of Applied Mechanics, IIT Delhi, Hauz Khas, New Delhi 110016, India

Received 22 March 2003; received in revised form 14 August 2003

Abstract

A new efficient higher order zigzag theory is presented for thermal stress analysis of laminated beams under thermal loads, with modification of the third order zigzag model by inclusion of the explicit contribution of the thermal expansion coefficient α_3 in the approximation of the transverse displacement w. The thermal field is approximated as piecewise linear across the thickness. The displacement field is expressed in terms of the thermal field and only three primary displacement variables by satisfying exactly the conditions of zero transverse shear stress at the top and the bottom and its continuity at the layer interfaces. The governing equations are derived using the principle of virtual work. Fourier series solutions are obtained for simply-supported beams. Comparison with the exact thermo-elasticity solution for thermal stress analysis under two kinds of thermal loads establishes that the present zigzag theory is generally very accurate and superior to the existing zigzag theory for composite and sandwich beams.

Keywords: Zigzag theory; Thermal load; Composite beam; Sandwich beam; Exact solution; Third order theory

1. Introduction

Laminated composite and sandwich structural elements are increasingly finding use as primary structural components, since they have excellent strength to weight and stiffness to weight ratio. But these have relatively poor strength and stiffness for transverse shear. Their failure mechanisms are strongly dependent on the local effects at the layer interfaces where the elastic moduli differ widely. Rational design of composite and sandwich beams, plates and shells requires accurate description of the in-plane stresses, transverse shear stresses and warping and straining of the normal to the mid-surface. The composite and sandwich structural components used in aerospace, underwater and land based structures are often subjected to moderate to severe environment or process based thermal loading causing significant thermal stresses due to thermal gradient across the thickness as well as due to widely different thermal properties of the adjacent laminas. The transverse shear plays a significant role for moderately thick and thick composite

* Corresponding author. Tel.: +91-11-26591218; fax: +91-11-26581119.
E-mail address: kapuria@am.iitd.ac.in (S. Kapuria).

0020-7683/$ - see front matter © 2003 Elsevier Ltd. All rights reserved.
doi:10.1016/j.ijsolstr.2003.08.014

and sandwich structures, since their transverse shear moduli are much smaller compared to the in-plane Young's moduli. Moreover, the layerwise inhomogeneity in the material properties causes a severe layerwise distortion of the normal to the mid-surface for the moderately thick and thick beams. As the first order shear deformation theory (FSDT) is inadequate to account for this distortion, several higher order theories have been developed. This work presents a new efficient higher order zigzag theory (HZIGT) for thermal stress analysis of composite and sandwich beams.

The classical laminate theory (CLT), the FSDT and the cubic third order theory (TOT) (Bickford, 1982; Reddy, 1984; Heyliger and Reddy, 1988) for laminated beams and plates under mechanical loading, have been covered in detail in Reddy (1997). Various higher order theories (HOTs) with Taylor series type expansions in the thickness direction z for the displacements have been developed for composite and sandwich beams (Kant and Manjunath, 1989, 1990; Soldatos and Elishakoff, 1992; Marur and Kant, 1997). CLT, FSDT, TOTs and HOTs are equivalent single layer (ESL) theories, in which the functional form of the displacement expansions is independent of the material properties of the layers, with the number of primary displacement unknowns independent of the number of layers. In these theories, the slope discontinuity in the in-plane displacements and shear stress continuity at the layer interfaces, as observed in the exact elasticity solution, are violated.

To overcome the deficiencies of the ESL theories, discrete layer theories (DLTs) have been developed for beams and plates with layerwise expansions of displacements with slope discontinuity in the in-plane displacements at the layer interfaces (Rao, 1978; Di Sciuva, 1986; Savoia et al., 1993). The DLTs which are only displacement-based do not satisfy the shear stress continuity conditions at the layer interfaces. The DLTs are more accurate than the ESLs, but are computationally expensive for real structural analysis since the number of displacement variables depends on the number of layers. To overcome this, zigzag theories have been developed for composite laminates in which the slope discontinuity in in-plane displacements at the layer interfaces is introduced through a zigzag function with values of $+1$ and -1 at successive layer interfaces (Li and Liu, 1995). More consistent efficient zigzag theories have been developed with layerwise expansion of displacements in which the number of primary displacement unknowns is reduced to those of the ESL theory of the same order, by imposing the conditions on the continuity of transverse shear stresses at the layer interfaces and by also possibly imposing the shear traction-free conditions at the top and the bottom surfaces. These zigzag theories are generalised 'equivalent single layer theories' with the expansion of the displacements having a functional form dependent on the material properties of the layers and their thicknesses. The accuracy of the zigzag theories is often comparable to that of the DLTs and the efficiency is comparable to that of the ESL theories. Several such zigzag theories (Cho and Parmerter, 1993; Averill and Yip, 1996; Aitharaju and Averill, 1999; Icardi, 2001) have been developed for static and dynamic analyses of beams and plates using polynomial expansion for displacements. Carrera (2001) has reviewed efficient zigzag theories using mixed formulations for displacements and stresses. Soldatos and his coworkers have developed generalised 'equivalent single layer theories' (Soldatos and Watson, 1997; Shu and Soldatos, 2000; Soldatos and Liu, 2001) for plates and beams with expansion of the displacements using shape functions obtained from the exact solution of the elasticity equations for the simply-supported boundary conditions, which satisfy shear traction-free conditions and the shear continuity conditions. These theories yield exact solutions for the simply-supported boundary conditions (Liu and Soldatos, 2002) and very accurate solutions for other boundary conditions.

Some of these theories have been extended to incorporate thermal loading. CLT (Tanigawa et al., 1989), FSDT and TOT (Reddy, 1997) have been developed for thermal stress analysis of beams and plates. Xioping and Liangxin (1994) developed an efficient zigzag model under thermal loading for composite plates with in-plane displacements expanded as a combination of a global cubic variation and layerwise linear variation of the type in Cho and Parmerter (1993). Ali et al. (1999) extended the zigzag theory of Li and Liu (1995) for thermo-mechanical analysis of plates. Noor and Malik (2000) used a predictor–corrector approach for plates under thermal loading using layerwise displacement field obtained for the

3D model for simply-supported edges to generate coordinate functions for the Rayleigh–Ritz technique and then adaptively refining them. Park and Kim (2002) presented a two step predictor–corrector procedure for finite element based thermal stress analysis of laminated plates using FSDT as a predictor. Carrera (2002) has presented a variety of displacement-based ESL theories and DLTs, and also mixed stress and displacement-based DLTs for thermal stress analysis of plates and assessed them for assumed linear temperature profile across the thickness and an actual temperature profile based on heat conduction equation. It was concluded that: (1) the ESL theories, in which the displacement expansions are independent of material properties, yield inaccurate results even for thin beams and plates; (2) the advanced zigzag theories may work well in thick plates loaded by assumed linear temperature profile but yield inaccurate results for actual temperature profile based on heat conduction equation; (3) at least a quadratic layerwise variation of w with z is required to capture even the linear thermal strain in the thickness direction. Soldatos and Liu (2003) have extended their generalised ESL theory for thermal loading of laminated beams. Exact thermo-elastic solutions (Bhaskar et al., 1996) reveal that the transverse displacement w is nonuniform across the thickness, primarily due to the transverse normal strain ε_{zz} caused by the temperature rise through the thermal expansion coefficient α_3. Except for the DLTs in which layerwise expansion is taken for w, no other available theory includes this transverse thermal strain which has enormous bearing on the results.

A new efficient 1D HZIGT is developed in this work for thermal stress analysis of composite and sandwich beams, with modification of the existing zigzag thermal model (Xioping and Liangxin, 1994) for plates by inclusion of the explicit contribution of the transverse thermal expansion coefficient α_3 in the approximation of the transverse displacement w. The axial displacement is approximated as a combination of a global third order variation across the thickness with an additional layerwise linear variation. The thermal field is approximated sub-layerwise as piecewise linear. The displacement field is expressed in terms of only three primary displacement variables and the thermal field by satisfying exactly the conditions of zero transverse shear stress at the top and the bottom surface of the beam and its continuity at the layer interfaces. The equilibrium equations and the boundary conditions are derived using the principle of virtual work. The number of primary displacement unknowns is three, which is independent of the number of layers and equal in number to the ones used in the FSDT and the TOT. This layerwise theory for displacement thus preserves the computational advantage of an ESL theory. Analytical Fourier series solutions are obtained for the response of simply-supported beams under thermal loads. The existing zigzag theory (ZIGT) for beams of the type given for plates by (Xioping and Liangxin, 1994) is obtained as a particular case of the present theory by setting $\alpha_3 = 0$ for all the layers. The present HZIGT is assessed by comparison with the exact 2D thermo-elasticity solution and the existing ZIGT, TOT and FSDT solutions. Numerical results for the displacements and the stresses for a benchmark test beam devised for this study, composite symmetric and anti-symmetric cross-ply laminated beams and sandwich beams establish that the present HZIGT is much superior to the existing theories.

2. Displacement approximations of higher order zigzag theory

Consider a composite or sandwich beam (Fig. 1) of width b, thickness h and length a, made of L perfectly bonded orthotropic layers with longitudinal axis x, subjected to thermal load with no variation along the width b. The axis along the width is y. The mid-plane of the beam is chosen as xy-plane. The planes $z = z_0 = -h/2$ and $z = z_L = h/2$ are the bottom and the top surfaces of the beam. z-Coordinate of the bottom surface of the kth layer (numbered from the bottom) is denoted as z_{k-1} and its material symmetry direction 1 is at an angle θ_k to x-axis. The reference plane $z = 0$ either passes through or is the bottom surface of the k_0th layer. For a beam with a small width, for mathematical simplicity of the 1D theory, the assumptions made by the other researchers that are retained are: assume plane state of stress

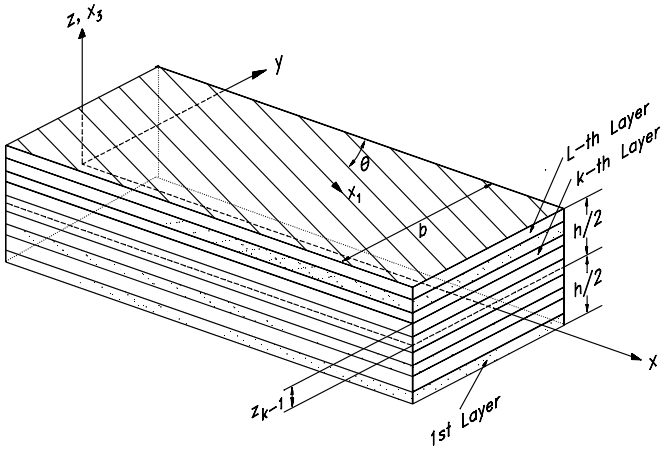

Fig. 1. Geometry of the laminated beam.

($\sigma_y = \tau_{yz} = \tau_{xy} = 0$), neglect transverse normal stress ($\sigma_z \simeq 0$) and assume the axial and transverse displacements u and w to be independent of y.

With these assumptions, using the strain–displacement relations for the strains ε_x, γ_{zx}; the stresses σ_x, τ_{zx} are related to the displacements by

$$\begin{aligned} \sigma_x &= \hat{Q}_{11}\varepsilon_x - \hat{\beta}_1\theta = \hat{Q}_{11}u_{,x} - \hat{\beta}_1\theta, \\ \tau_{zx} &= \hat{Q}_{55}\gamma_{zx} = \hat{Q}_{55}(u_{,z} + w_{,x}), \end{aligned} \tag{1}$$

where a subscript comma denotes differentiation and the expressions for the stiffness $\hat{Q}_{11}$, $\hat{Q}_{55}$ and the stress-temperature coefficient $\hat{\beta}_1$ can be expressed in terms of the Young's moduli Y_1, Y_2, shear moduli G_{55}, Poisson's ratio v_{12}, thermal expansion coefficients α_1, α_2 and the orientation of the principal material axes.

The 2D thermal problem for the beam, involving the heat conduction equation, can be solved analytically or by the finite element method for $\theta(x,z)$. For the model developed herein, θ is approximated as piecewise linear between its values $\theta(x,z_\theta^l)$ at n_θ points z_θ^l, $l = 1,2,\ldots,n_\theta$ across the thickness h:

$$\theta(x,z) = \Psi_\theta^l(z)\theta^l(x), \tag{2}$$

where $\theta^l(x) = \theta(x,z_\theta^l)$ and $\Psi_\theta^l(z)$ are linear interpolation functions and summation convention is used for index l. n_θ can differ from L with $n_\theta \geqslant L$ and is determined by the accuracy required of θ. The functional form of $\theta^l(x)$ will depend on the boundary conditions.

Two-dimensional thermo-elastic exact solutions (Bhaskar et al., 1996) have revealed that for moderately thick beams under thermal load, the deflection w has significant variation across the thickness as the thermal contribution to strain ε_z becomes much greater than the negligible contribution due to the stresses σ_x, σ_z. Hence, the deflection w is approximated by integrating the constitutive equation for ε_z by neglecting the contribution of elastic compliance, i.e., by including only the thermal contribution: $\varepsilon_z = w_{,z} \simeq \alpha_3\theta \Rightarrow$

$$w(x,z) = w_0(x) + \bar{\Psi}_\theta^l(z)\theta^l(x) \tag{3}$$

where $\bar{\Psi}_\theta^l(z) = \int_0^z \alpha_3 \Psi_\theta^l(z)\,\mathrm{d}z$ is a piecewise quadratic function.

The axial displacement is assumed (Xioping and Liangxin, 1994) as a combination of a third order variation across the thickness with a layerwise linear variation. For the kth layer, u is assumed as

$$u(x,z) = u_k(x) - zw_{0,x}(x) + z\psi_k(x) + z^2\xi(x) + z^3\eta(x), \tag{4}$$

where u_k and ψ_k denote translation and rotation variables of the kth layer. Substituting u and w from Eqs. (4) and (3) into Eq. (1) yields

$$\tau_{zx} = \hat{Q}^k_{55}(\psi_k + 2z\xi + 3z^2\eta) + \hat{Q}^k_{55}\bar{\Psi}^l_\theta(z)\theta^l_{,x}. \tag{5}$$

For the k_0th layer, denote $u_0(x) = u_{k_0}(x) = u(x,0)$, $\psi_0(x) = \psi_{k_0}(x)$. The functions u_k, ψ_k, ξ, η are expressed in terms of u_0 and ψ_0 using the $(L-1)$ conditions each for the continuity of τ_{zx} and u at the layer interfaces and the two shear traction-free conditions $\tau_{zx} = 0$ at the top and the bottom surfaces at $z = z_0, z_L$. The continuity of τ_{zx} at the interface $z = z_{i-1}$ between the layers i and $i-1$ yields

$$\hat{Q}^i_{55}[\psi_i + 2z_{i-1}\xi + 3z^2_{i-1}\eta] + \hat{Q}^i_{55}\bar{\Psi}^l_\theta(z_{i-1})\theta^l_{,x} = \hat{Q}^{i-1}_{55}[\psi_{i-1} + 2z_{i-1}\xi + 3z^2_{i-1}\eta] + \hat{Q}^{i-1}_{55}\bar{\Psi}^l_\theta(z_{i-1})\theta^l_{,x}. \tag{6}$$

Eq. (6) is written in the following recursive form so that the solution of ψ_i, ξ, η is easily tractable:

$$\begin{aligned}
&\hat{Q}^i_{55}[\psi_i + 2z_i\xi + 3z^2_i\eta] + \hat{Q}^i_{55}\bar{\Psi}^l_\theta(z_i)\theta^l_{,x} \\
&\quad = \hat{Q}^{i-1}_{55}[\psi_{i-1} + 2z_{i-1}\xi + 3z^2_{i-1}\eta] + \hat{Q}^{i-1}_{55}\bar{\Psi}^l_\theta(z_{i-1})\theta^l_{,x} + 2\hat{Q}^i_{55}(z_i - z_{i-1})\xi + 3\hat{Q}^i_{55}(z^2_i - z^2_{i-1})\eta \\
&\qquad + \hat{Q}^i_{55}[\bar{\Psi}^l_\theta(z_i) - \bar{\Psi}^l_\theta(z_{i-1})]\theta^l_{,x}.
\end{aligned} \tag{7}$$

Using Eq. (5), $\tau_{zx}(x, z_0) = 0$, can also be written in the above pattern as

$$\hat{Q}^1_{55}[\psi_1 + 2z_1\xi + 3z^2_1\eta] + \hat{Q}^1_{55}\bar{\Psi}^l_\theta(z_1)\theta^l_{,x} = 2\hat{Q}^1_{55}(z_1 - z_0)\xi + 3\hat{Q}^1_{55}(z^2_1 - z^2_0)\eta + \hat{Q}^1_{55}[\bar{\Psi}^l_\theta(z_1) - \bar{\Psi}^l_\theta(z_0)]\theta^l_{,x}. \tag{8}$$

Adding Eq. (8) and Eq. (7) for $i = 2, 3, \ldots, k$ yields

$$\hat{Q}^k_{55}(\psi_k + 2z_k\xi + 3z^2_k\eta) + \hat{Q}^k_{55}\bar{\Psi}^l_\theta(z_k)\theta^l_{,x} = 2C^k_1\xi + 6C^k_2\eta + C^k_{3l}\theta^l_{,x}, \quad k = 2, \ldots, L, \tag{9}$$

where

$$C^k_1 = \sum_{i=1}^{k}\hat{Q}^i_{55}(z_i - z_{i-1}), \quad C^k_2 = \sum_{i=1}^{k}\hat{Q}^i_{55}(z^2_i - z^2_{i-1})/2, \quad C^k_{3l} = \sum_{i=1}^{k}\hat{Q}^i_{55}[\bar{\Psi}^l_\theta(z_i) - \bar{\Psi}^l_\theta(z_{i-1})]. \tag{10}$$

Using Eq. (5), the condition $\tau_{zx}(x, z_L) = 0$, can be written as

$$\hat{Q}^L_{55}[\psi_L + 2z_L\xi + 3z^2_L\eta] + \hat{Q}^L_{55}\bar{\Psi}^l_\theta(z_L)\theta^l_{,x} = 0. \tag{11}$$

Eliminating ψ_L from Eq. (11) and (9) for $k = L$, and rewriting Eq. (8) yields

$$2C^L_1\xi + 6C^L_2\eta = -C^L_{3l}\theta^l_{,x}, \quad 2z_0\xi + 3z^2_0\eta = C^l_5\theta^l_{,x} - \psi_1 \tag{12}$$

where $C^l_5 = -\bar{\Psi}^l_\theta(z_0)$. The solution of ξ, η from Eq. (12) is

$$\xi = R_3\psi_1 + R^l_5\theta^l_{,x}, \quad \eta = R_4\psi_1 + R^l_6\theta^l_{,x}, \tag{13}$$

$$\begin{aligned}
&R_3 = 4C^L_2/\Delta, \quad R^l_5 = -(2z^2_0C^L_{3l} + 4C^L_2C^L_5)/\Delta, \\
&R_4 = -4C^L_1/3\Delta, \quad R^l_6 = (4z_0C^L_{3l} + 4C^L_1C^l_5)/3\Delta,
\end{aligned} \tag{14}$$

with $\Delta = 4z^2_0C^L_1 - 8z_0C^L_2$. Substituting ξ, η from Eq. (13) into Eq. (9) yields

$$\psi_k = R^k_2\psi_1 + R^k_{l1}\theta^l_{,x}, \tag{15}$$

$$\begin{aligned}
&R^k_2 = a^k_1R_3 + a^k_2R_4, \quad a^k_1 = 2(C^k_1/\hat{Q}^k_{55} - z_k), \\
&R^k_{l1} = a^k_1R^l_5 + a^k_2R^l_6 + C^k_{3l}/\hat{Q}^k_{55} - \bar{\Psi}^l_\theta(z_k), \quad a^k_2 = 3(2C^k_2/\hat{Q}^k_{55} - z^2_k).
\end{aligned} \tag{16}$$

Using Eq. (4), continuity of u between layers i and $i-1 \Rightarrow u_i + z_{i-1}\psi_i = u_{i-1} + z_{i-1}\psi_{i-1}$ and using Eq. (15):

$$u_i = u_{i-1} + z_{i-1}[(R_2^{i-1} - R_2^i)\psi_1 + (R_{l1}^{i-1} - R_{l1}^i)\theta_{,x}^l], \quad i = 2, \ldots, L. \tag{17}$$

Adding Eq. (17) for $i = 2$ to k yields u_k in terms of u_1:

$$u_k = u_1 + \bar{R}_2^k \psi_1 + \bar{R}_{l1}^k \theta_{,x}^l, \tag{18}$$

$$\bar{R}_2^k = \sum_{i=2}^{k} z_{i-1}(R_2^{i-1} - R_2^i), \quad \bar{R}_{l1}^k = \sum_{i=2}^{k} z_{i-1}(R_{l1}^{i-1} - R_{l1}^i). \tag{19}$$

Eqs. (18) and (15) yield for the k_0th layer:

$$u_0(x) = u_{k_0}(x) = u_1 + \bar{R}_2^{k_0}\psi_1 + \bar{R}_{l1}^{k_0}\theta_{,x}^l, \tag{20}$$

$$\psi_0(x) = \psi_{k_0}(x) = R_2^{k_0}\psi_1 + R_{l1}^{k_0}\theta_{,x}^l. \tag{21}$$

Substituting ξ, η from Eq. (13), u_k from Eq. (18) with u_1 from Eq. (20) and ψ_k from Eq. (15) in Eq. (4) yields

$$u(x,z) = u_0(x) - z w_{0,x}(x) + R_k(z)\psi_1(x) + R_{k\theta}^l(z)\theta_{,x}^l, \tag{22}$$

where

$$\begin{aligned} &R_k(z) = R_1^k + zR_2^k + z^2R_3 + z^3R_4, \quad R_1^k = \bar{R}_2^k - \bar{R}_2^{k_0}, \\ &R_{k\theta}^l(z) = R_1^{kl} + zR_{l1}^k + z^2R_5^l + z^3R_6^l, \quad R_1^{kl} = \bar{R}_{l1}^k - \bar{R}_{l1}^{k_0}. \end{aligned} \tag{23}$$

Substituting ψ_1 in terms of ψ_0 from Eq. (21) into Eq. (22) yields the expression of u as

$$u(x,z) = u_0(x) - z w_{0,x}(x) + R^k(z)\psi_0(x) + \bar{R}^{kl}(z)\theta_{,x}^l(x), \tag{24}$$

where

$$\begin{aligned} &R^k(z) = R_k(z)/R_2^{k_0} = \hat{R}_1^k + z\hat{R}_2^k + z^2\hat{R}_3 + z^3\hat{R}_4, \\ &\bar{R}^{kl}(z) = R_{k\theta}^l(z) - R_k(z)R_{l1}^{k_0}/R_2^{k_0} = \hat{R}_1^{kl} + z\hat{R}_{l1}^k + z^2\hat{R}_5^l + z^3\hat{R}_6^l, \end{aligned} \tag{25}$$

$$\begin{aligned} &(\hat{R}_1^k, \hat{R}_2^k, \hat{R}_3^k, \hat{R}_4^k) = (R_1^k, R_2^k, R_3^k, R_4^k)/R_2^{k_0}, \quad \hat{R}_5^l = R_5^l - \hat{R}_3 R_{l1}^{k_0}, \\ &\hat{R}_1^{kl} = R_1^{kl} - \hat{R}_1^k R_{l1}^{k_0}, \quad \hat{R}_{l1}^k = R_{l1}^k - \hat{R}_2^k R_{l1}^{k_0}, \quad \hat{R}_6^l = R_6^l - \hat{R}_4 R_{l1}^{k_0}. \end{aligned} \tag{26}$$

Thus w, u are expressed by Eqs. (3) and (24) in terms of the primary variables u_0, w_0, ψ_0 which are the same as in the FSDT.

3. Governing equations of HZIGT

Using the notation $\langle \ldots \rangle = \sum_{k=1}^{L} \int_{z_{k-1}^+}^{z_k^-} (\ldots) b \, dz$, define the following stress resultants:

$$[N_x, M_x, P_x] = \langle [1, z, R^k(z)]\sigma_x \rangle, \quad [Q_x, V_x] = \langle [R_{,z}^k(z), 1]\tau_{zx} \rangle, \tag{27}$$

Using the principle of virtual work and the expressions of δu, δw in terms of δu_0, δw_0, $\delta\psi_0$ from Eqs. (24) and (3), yields three equilibrium equations in terms of the force resultants and four boundary conditions at each end. The details are omitted for brevity. The equilibrium equations are

$$N_{x,x} = 0, \quad M_{x,xx} = 0, \quad P_{x,x} - Q_x = 0. \tag{28}$$

The boundary conditions at the ends at $x = 0, a$ are

$$\begin{aligned} &u_0 = \bar{u}_0 \quad \text{or} \quad N_x = \bar{N}_x, \qquad w_{0,x} = \bar{w}_{0,x} \quad \text{or} \quad M_x = \bar{M}_x, \\ &\psi_0 = \bar{\psi}_0 \quad \text{or} \quad P_x = \bar{P}_x, \qquad w_0 = \bar{w}_0 \quad \text{or} \quad M_{x,x} = \bar{V}_x, \end{aligned} \tag{29}$$

where an over-bar denotes a prescribed value.

Substituting θ, w, u from Eqs. (2), (3) and (24) in Eq. (1) and substituting these expressions of σ_x, τ_{zx} in Eq. (27) yields the following expressions of the force resultants in terms of the primary displacements:

$$\begin{bmatrix} N_x \\ M_x \\ P_x \end{bmatrix} = \begin{bmatrix} A_{11} & A_{12} & A_{13} \\ A_{12} & A_{22} & A_{23} \\ A_{13} & A_{23} & A_{33} \end{bmatrix} \begin{bmatrix} u_{0,x} \\ -w_{0,xx} \\ \psi_{0,x} \end{bmatrix} + \begin{bmatrix} A_1^l \\ A_2^l \\ A_3^l \end{bmatrix} \theta^l_{,xx} - \begin{bmatrix} \gamma_1^l \\ \gamma_2^l \\ \gamma_3^l \end{bmatrix} \theta^l, \tag{30a}$$

$$Q_x = \bar{A}_{33}\psi_0 + \bar{A}_3^l \theta^l_{,x}, \tag{30b}$$

where the beam stiffness A_{ij}, $\bar{A}_{ij}$; the beam thermal stiffness γ_i^l, the beam thermo-mechanical coefficients A_i^l, $\bar{A}_i^l$; are defined in terms of the material parameters by

$$\begin{aligned} &[A_{11}, A_{12}, A_{13}, A_1^l] = \langle \hat{Q}_{11}[1, z, R^k(z), \bar{R}^{kl}(z)] \rangle, \quad [A_{33}, A_3^l] = \langle \hat{Q}_{11} R^k(z)[R^k(z), \bar{R}^{kl}(z)] \rangle, \\ &[A_{22}, A_{23}, A_2^l] = \langle \hat{Q}_{11} z[z, R^k(z), \bar{R}^{kl}(z)] \rangle, \quad [\gamma_1^l, \gamma_2^l, \gamma_3^l] = \langle \hat{\beta}_1 \Psi^l_\theta(z)[1, z, R^k(z)] \rangle, \\ &[\bar{A}_{33}, \bar{A}_3^l] = \langle \hat{Q}_{55} R^k_{,z}(z)[R^k_{,z}(z), \bar{R}^{kl}_{,z}(z) + \bar{\Psi}^l_\theta(z)] \rangle. \end{aligned} \tag{31}$$

The equilibrium equations are expressed in terms of the primary variables u_0, w_0, ψ_0 by substitution of the expressions of the stress resultants from Eq. (30) into Eq. (28):

$$\begin{aligned} &-A_{11}u_{0,xx} + A_{12}w_{0,xxx} - A_{13}\psi_{0,xx} = A_1^l \theta^l_{,xxx} - \gamma_1^l \theta^l_{,x}, \\ &-A_{12}u_{0,xxx} + A_{22}w_{0,xxxx} - A_{23}\psi_{0,xxx} = A_2^l \theta^l_{,xxxx} - \gamma_2^l \theta^l_{,xx}, \\ &-A_{13}u_{0,xx} + A_{23}w_{0,xxx} - A_{33}\psi_{0,xx} + \bar{A}_{33}\psi_0 = A_3^l \theta^l_{,xxx} - (\gamma_3^l + \bar{A}_3^l)\theta^l_{,x}. \end{aligned} \tag{32}$$

The stress τ_{zx} can be obtained using constitutive equation (1) directly or more accurately by integrating the 2D equation of equilibrium in x-direction to yield $\tau_{zx} = -\int_{-h/2}^{z} \sigma_{x,x}\, dz$.

In order to assess the accuracy of the theory developed herein, analytical linear solution is obtained for simply-supported beams with the following boundary conditions at $x = 0, a$:

$$N_x = 0, \quad w_0 = 0, \quad M_x = 0, \quad P_x = 0, \quad \theta = 0. \tag{33}$$

The solution of Eq. (32) is expanded in the following Fourier series,which satisfy the boundary conditions (33) at the ends:

$$(w_0, N_x, M_x, P_x, \theta) = \sum_{n=1}^{\infty} (w_0, N_x, M_x, P_x, \theta)_n \sin \bar{n}x, \quad (u_0, \psi_0, Q_x) = \sum_{n=1}^{\infty} (u_0, \psi_0, Q_x)_n \cos \bar{n}x, \tag{34}$$

with $\bar{n} = n\pi/a$. Substituting these in Eq. (32), yields for the nth Fourier component, following linear algebraic equations:

$$K\bar{U}^n = \bar{P}^n, \tag{35}$$

where $\bar{U}^n = [\, u_0 \quad w_0 \quad \psi_0 \,]_n^{\mathrm{T}}$ is the displacement vector, $\bar{P}^n = [\, P_1 \quad P_2 \quad P_3 \,]_n^{\mathrm{T}}$ is the thermal load vector and K is the symmetric stiffness matrix with

$$
\begin{aligned}
&K_{11} = \bar{n}^2 A_{11}, \quad K_{12} = -\bar{n}^3 A_{12}, \quad K_{13} = \bar{n}^2 A_{13},\\
&K_{22} = \bar{n}^4 A_{22}, \quad K_{23} = \bar{n}^3 A_{23}, \quad K_{33} = \bar{n}^2 A_{33} + \bar{A}_{33},\\
&P_1 = -(\bar{n}^3 A_1^l + \bar{n}\gamma_1^l)\theta_n^l, \quad P_2 = (\bar{n}^4 A_2^l + \bar{n}^2\gamma_2^l)\theta_n^l, \quad P_3 = -[\bar{n}^3 A_3^l + \bar{n}(\gamma_3^l + \bar{A}_3^l)]\theta_n^l.
\end{aligned} \tag{36}
$$

4. Numerical results and assessment

The accuracy of the present theory is assessed by comparison with the exact 2D thermo-elasticity solution (Bhaskar et al., 1996). The results are also compared with the existing zigzag theory, TOT and FSDT in order to assess its improvement over these theories. The shear correction factor for the FSDT solution is taken as 5/6. Four highly inhomogeneous simply-supported beams (a)–(d) are selected for the numerical

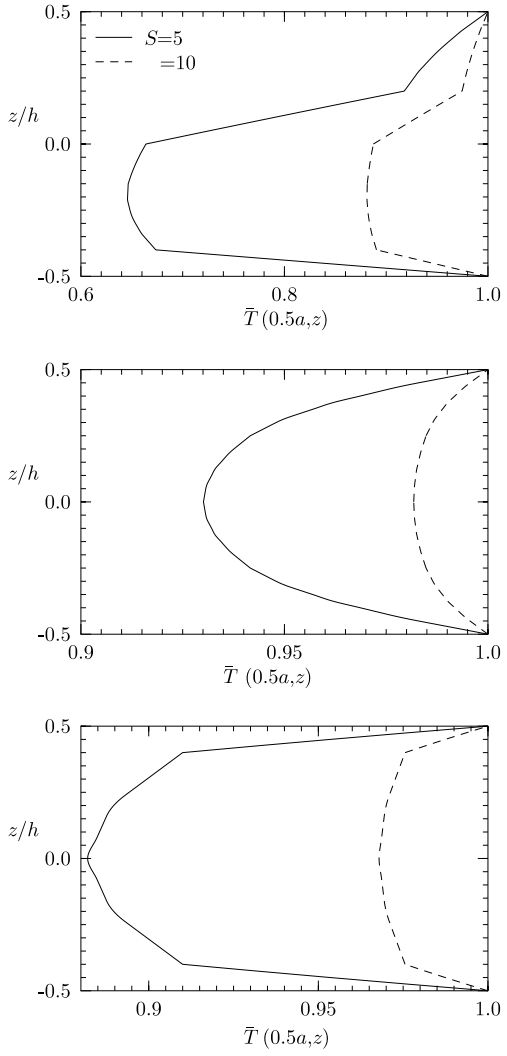

Fig. 2. Temperature distribution for beams (a), (b) and (d) under load case 1.

study. The stacking order is mentioned from the bottom. The 5-ply beam (a), which has been devised as a benchmark test case, has plys of thickness $0.1h/0.25h/0.15h/0.2h/0.3h$ of materials 1/2/3/1/3 which have highly inhomogeneous properties for stiffness in tension and shear as in Averill and Yip (1996) and highly inhomogeneous coefficients of thermal expansion and thermal conductivities. Beams (b) and (c) are graphite-epoxy composite beams of material 4 (Xu et al., 1995), consisting of four plys of equal thickness $0.25h$ with symmetric [0°/90°/90°/0°] and anti-symmetric [90°/0°/90°/0°] lay-ups respectively. The three-layer sandwich beam (d) has graphite-epoxy faces and a soft core (Noor and Burton, 1994) with thickness $0.1h/0.8h/0.1h$. The orientation $\theta_k = 0$ for all the plys of beams (a) and (d). The material properties of materials 1–4 and of the face of the sandwich beam are: $[(Y_L, Y_T, G_{LT}, G_{TT}), \nu_{LT}, \nu_{TT}, (\alpha_L, \alpha_T)(k_L, k_T)] =$

Material 1: [(6.9, 6.9, 1.38, 1.38) GPa, 0.25, 0.25, (35.6, 35.6)$\times 10^{-6}$ K^{-1}, (0.12, 0.12) W_{m}^{-1} K^{-1}]

Material 2: [(224.25, 6.9, 56.58, 1.38) GPa, 0.25, 0.25, (0.25, 35.6)$\times 10^{-6}$ K^{-1}, (7.2, 1.44) W_{m}^{-1} K^{-1}]

Material 3: [(172.5, 6.9, 3.45, 1.38) GPa, 0.25, 0.25, (0.57, 35.6)$\times 10^{-6}$ K^{-1}, (1.92, 0.96) W_{m}^{-1} K^{-1}]

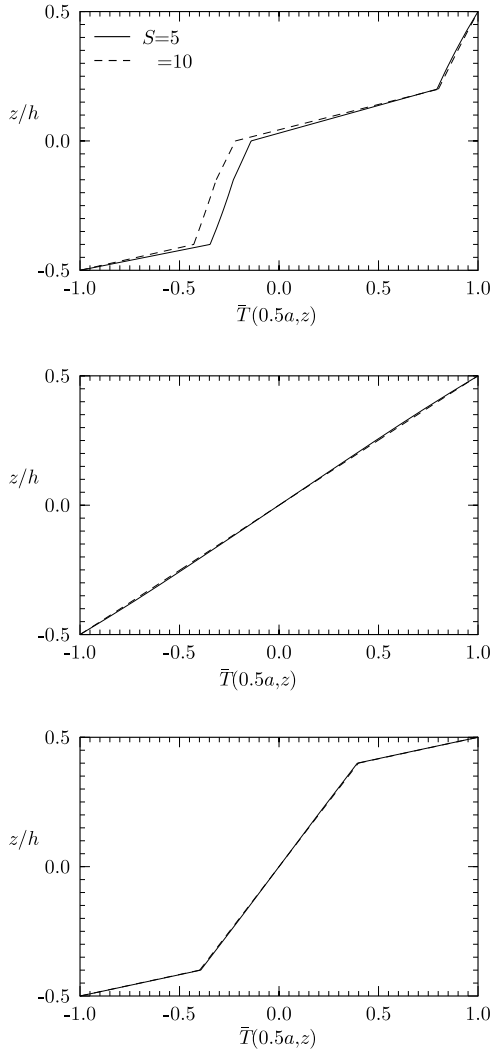

Fig. 3. Temperature distribution for beams (a), (b) and (d) under load case 2.

Material 4: [(181, 10.3, 7.17, 2.87) GPa, 0.28, 0.33, (0.02, 22.5)$\times 10^{-6}$ K^{-1}, (1.5, 0.5) W_{m}^{-1} K^{-1}]
Face: [(131.1, 6.9, 3.588, 2.3322) GPa, 0.32, 0.49, (0.0225, 22.5)$\times 10^{-6}$ K^{-1}, (1.5, 0.5) W_{m}^{-1} K^{-1}]
For the core: $[(Y_1, Y_2, Y_3, G_{12}, G_{23}, G_{31}), \nu_{12}, \nu_{13}, \nu_{23}] = [(0.2208, 0.2001, 2760, 16.56, 455.4, 545.1)$ MPa, $0.99, 3\times 10^{-5}, 3\times 10^{-5}]$, $\alpha_i = 30.6\times 10^{-6}$ K^{-1}, $k_i = 3.0$ W_{m}^{-1} K^{-1},

where L and T denote directions parallel and transverse to the fibres, ν_{LT} is Poisson's ratio for strain in T-direction under uniaxial normal stress in L-direction, and k_L, k_T, k_i are the thermal conductivity coefficients.

Two thermal load cases are considered.

1. Equal temperature rise of the bottom and the top surfaces of the beam with sinusoidal longitudinal variation: $\theta(x, \pm h/2) = T_0 \sin(n\pi x/a)$.
2. Equal rise and fall of temperature of the top and bottom surfaces of the beam with sinusoidal longitudinal variation: $\theta(x, h/2) = -\theta(x, -h/2) = T_0 \sin(n\pi x/a)$.

For the symmetric laminate, case 1 corresponds to thermal extension problem with no deflection of the mid-surface and case 2 corresponds to thermal bending problem with no extension of the mid-surface. The results are nondimensionalised as follows with $S = a/h$ and with the respective values of Y_T and α_T for beams (a)–(c) and those of the face material for beam (d):

$$(\bar{u}, \bar{w}) = 100(u, w/S)/\alpha_T S h T_0, \quad (\bar{\sigma}_x, \bar{\tau}_{zx}) = (\sigma_x, S\tau_{zx})/\alpha_T Y_T T_0, \quad \bar{T} = T/T_0.$$

The 2D thermal problem is solved exactly by exact analytical solution of the heat conduction equation for all the layers and exact satisfaction of the thermal boundary conditions at the ends at $x = 0, a$; at the top and bottom at $z = \pm h/2$; and the continuity conditions at the layer interfaces for temperature and heat flow. The distributions of temperature across the thickness, for case 1 of equal rise of temperature of the top and bottom of the beam, and for case 2 of equal rise and fall of the temperature of these surfaces, are depicted in Figs. 2 and 3, respectively. These cover a wide range of temperature profiles with large discontinuities in its slope at the layer interfaces in some cases and constitute ideal lay-ups and thermal load cases for assessment of 1D theories. The benchmark test beam (a), devised for this study, does indeed simulate the case of highly nonlinear temperature distribution with large discontinuities in its slope. For the present zigzag theory (HZIGT), each layer is divided into m sub-layers for the discretisation of the temperature field across the thickness. Hence, for a beam of L plys, the number n_θ of interpolation points in Eq. (2) equals $mL + 1$. The values of $\theta_l(x)$ used in Eq. (2) for piecewise linear discretisation of θ are obtained from the values θ^l of the 2D analytical thermal solution at these n_θ interpolation points, i.e., $\theta^l(x) = \theta^l \sin(n\pi x/a)$. Convergence studies have revealed that accurate results are obtained by approximating the exact temperature distributions across the thickness by sub-layerwise linear distributions with four equal sub-layers in each ply. As mentioned in the introduction, the ZIGT results are obtained from the formulation of HZIGT by setting $\alpha_3 = 0$ for all the layers.

The thickness distributions of $\bar{u}$, $\bar{\tau}_{zx}$ at the end and of $\bar{w}$, $\bar{\sigma}_x$ at the centre, obtained by the present zigzag theory (HZIGT), are compared with the exact 2D thermo-elasticity solution and the existing ZIGT in Fig. 4 for thermal load case 1 for thick ($S = 5$) and moderately thick ($S = 10$) test beam (a). Similar results for beams (b)–(d) for load case 1 are presented in Figs. 5–7, respectively. The results for the four beams for load case 2 are compared in Figs. 8–11. The distribution of $\bar{u}$ for the present HZIGT in Figs. 4 and 5 for test beam (a) and symmetric composite beam (b), under thermal load 1, have large qualitative and quantitative errors in the middle layers for $S = 5, 10$, whereas the existing zigzag theory ZIGT has large errors for all the layers. The corresponding errors in the $\bar{u}$ distributions for thermal load 2 in Figs. 8 and 9 are relatively much smaller. The $\bar{u}$ distributions of the present HZIGT for unsymmetric composite beam (c), for loads 1 and 2, agree quite well with the exact solution for the moderately thick beams with $S = 10$, but there is significant error for the thick beams with $S = 5$. The $\bar{u}$ distributions of the sandwich beam (d) for the

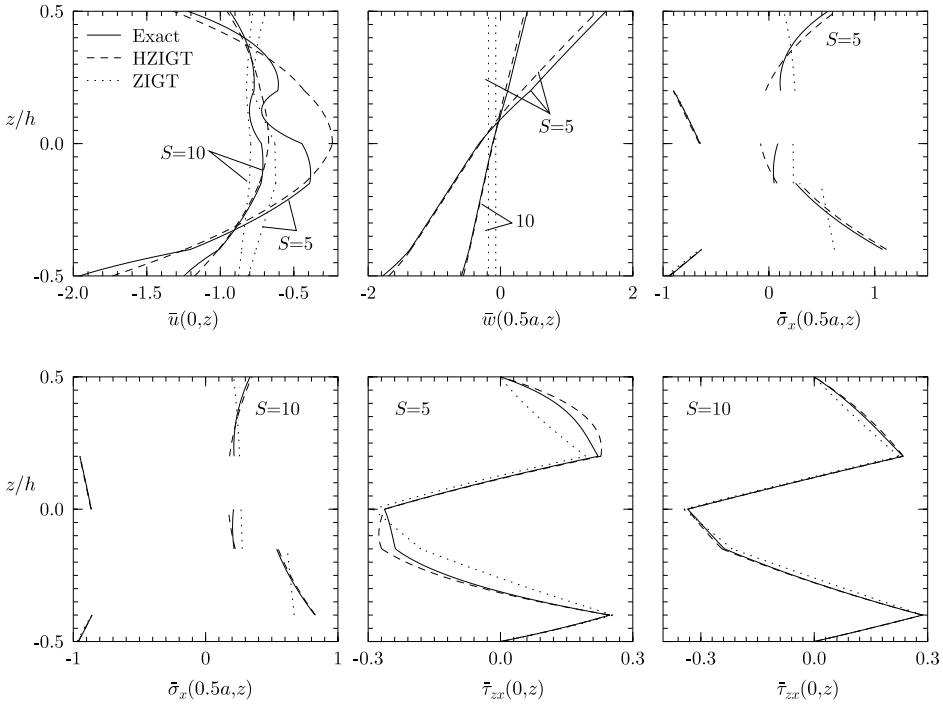

Fig. 4. Distributions of $\bar{u}$, $\bar{w}$, $\bar{\sigma}_x$, $\bar{\tau}_{zx}$ for test beam (a) under load case 1.

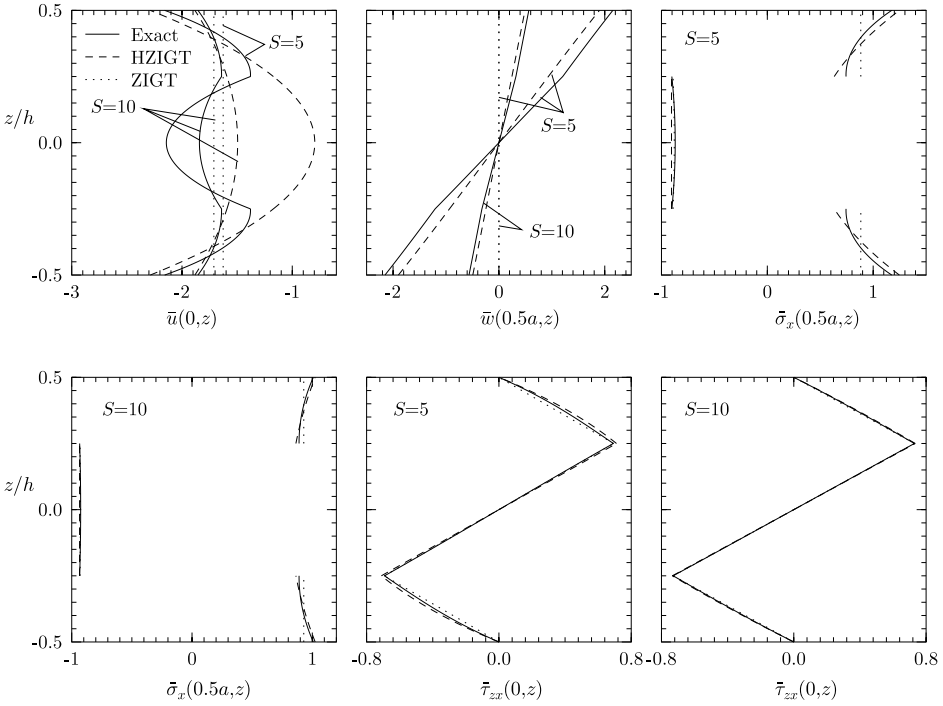

Fig. 5. Distributions of $\bar{u}$, $\bar{w}$, $\bar{\sigma}_x$, $\bar{\tau}_{zx}$ for composite beam (b) under load case 1.

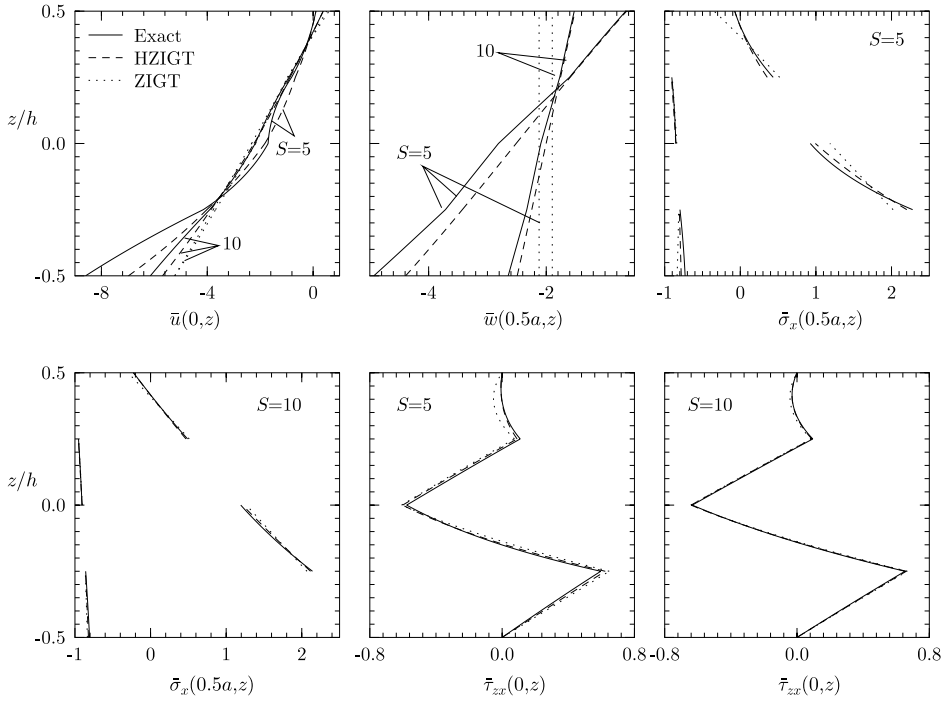

Fig. 6. Distributions of $\bar{u}$, $\bar{w}$, $\bar{\sigma}_x$, $\bar{\tau}_{zx}$ for composite beam (c) under load case 1.

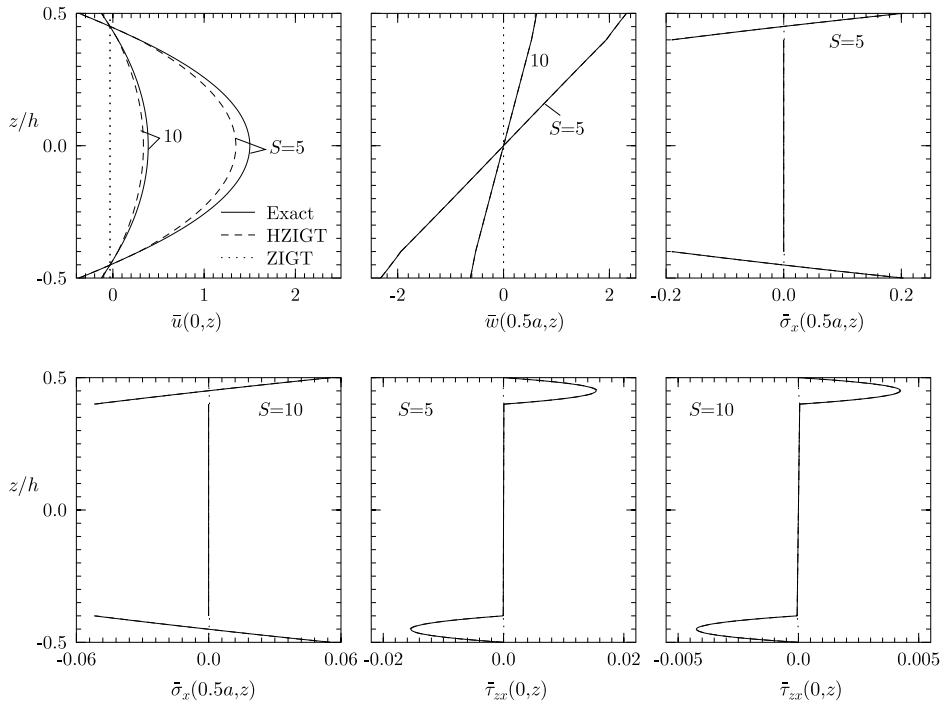

Fig. 7. Distributions of $\bar{u}$, $\bar{w}$, $\bar{\sigma}_x$, $\bar{\tau}_{zx}$ for sandwich beam (d) under load case 1.

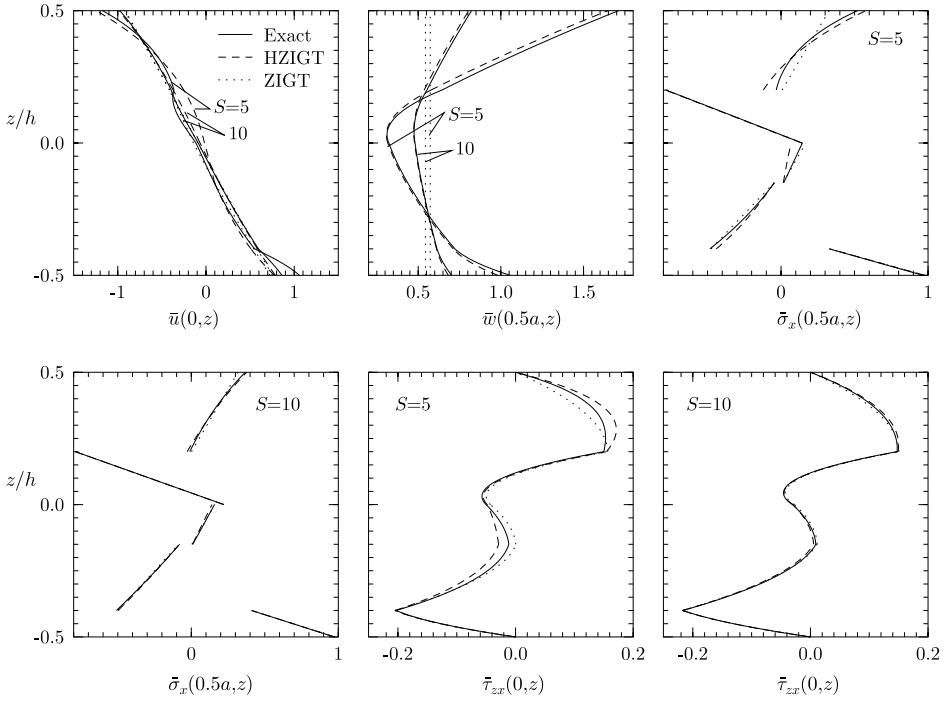

Fig. 8. Distributions of $\bar{u}$, $\bar{w}$, $\bar{\sigma}_x$, $\bar{\tau}_{zx}$ for test beam (a) under load case 2.

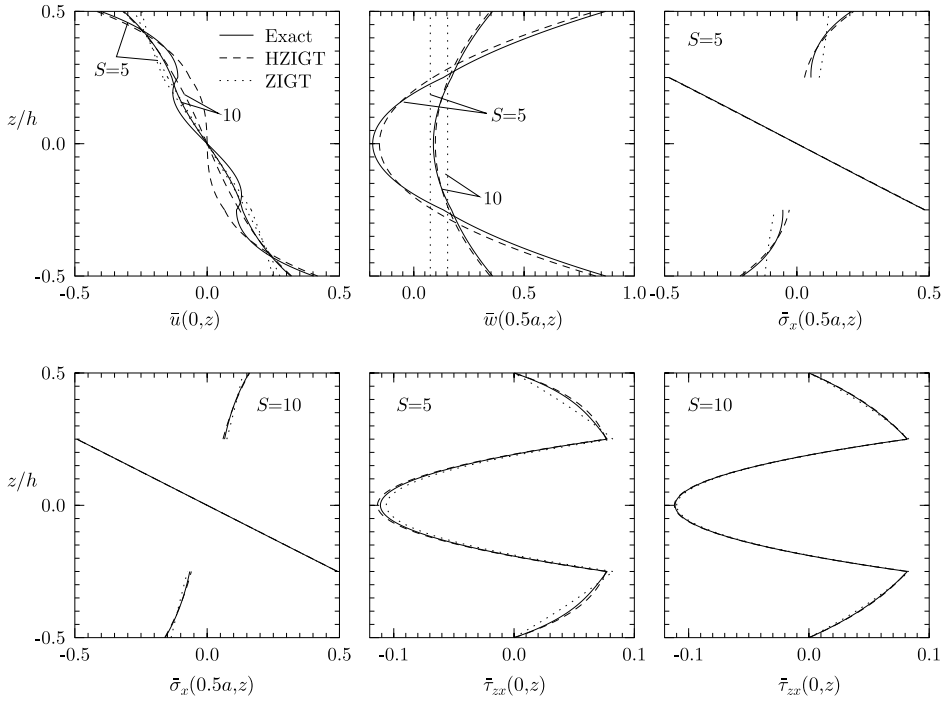

Fig. 9. Distributions of $\bar{u}$, $\bar{w}$, $\bar{\sigma}_x$, $\bar{\tau}_{zx}$ for composite beam (b) under load case 2.

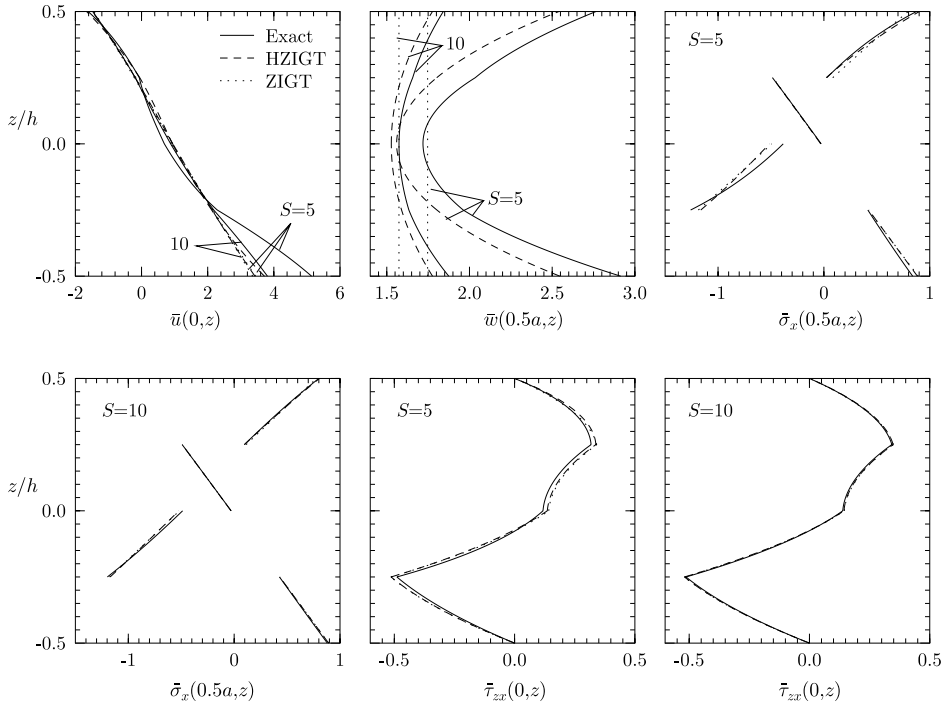

Fig. 10. Distributions of $\bar{u}$, $\bar{w}$, $\bar{\sigma}_x$, $\bar{\tau}_{zx}$ for composite beam (c) under load case 2.

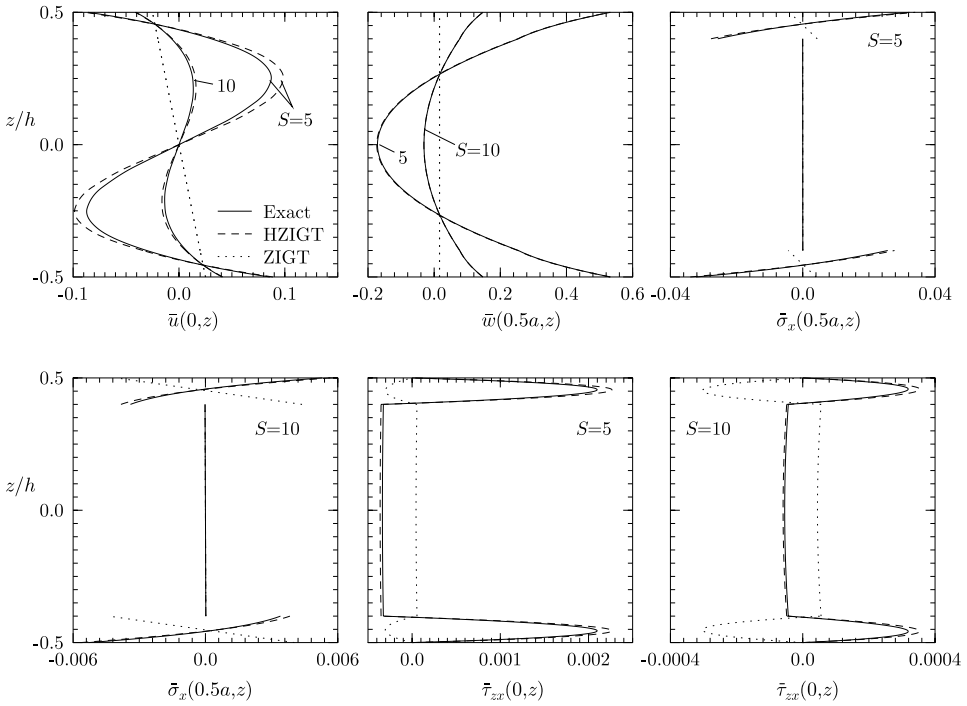

Fig. 11. Distributions of $\bar{u}$, $\bar{w}$, $\bar{\sigma}_x$, $\bar{\tau}_{zx}$ for sandwich beam (d) under load case 2.

present HZIGT, are in good qualitative and quantitative agreement with the exact solution for $S = 10, 5$ for both the load cases, whereas the existing ZIGT does not agree qualitatively and has large error. In all cases, the $\bar{u}$ distributions of the present HZIGT are more accurate than those of the existing ZIGT, with the maximum improvement for the sandwich beam (d) in both the load cases, and the least improvement for load case 1 for the symmetric composite beam (c).

The distributions of the transverse displacement $\bar{w}$ across the thickness for the present HZIGT are in excellent qualitative agreement with the exact 2D thermo-elasticity solution for all the beams with $S = 10, 5$ in both load cases, with small quantitative error. The uniform distributions of $\bar{w}$ for the existing ZIGT are highly erroneous for all the cases. The $\bar{w}$ distribution of the present HZIGT in both the load cases has the least error for the sandwich beam (d), while the maximum error in load case 1 is for the symmetric composite beam (b) and in load case 2 it is for the anti-symmetric composite beam (c).

The $\bar{\sigma}_x$ distributions for the present HZIGT, in both load cases, closely follow the pattern of the distributions for the exact 2D solutions for all the beams, except in one layer of the anti-symmetric beam (c) with $S = 5$ for load case 2 (Fig. 10). The distributions of $\bar{\sigma}_x$ obtained by the existing ZIGT are fairly good for some layers of beams (a)–(c) with large error in one, two or more layers for $S = 5$ and even for $S = 10$ for beams (a) and (b) under thermal load 1. For the sandwich beam (d), the error of the present HZIGT is very small, whereas the pattern of the existing ZIGT solution is totally wrong with large error in its two face layers. The distribution of post-processed $\bar{\tau}_{zx}$ obtained by the HZIGT and the ZIGT is quite good for all the beams, except the sandwich beam (d) for which the ZIGT solution has large errors for both the load cases.

The exact 2D thermo-elastic results for displacements and stresses at typical points across the thickness, where they are large, along with the % errors of the present HZIGT, existing ZIGT, TOT of the type given by Reddy (1984) and FSDT, are given in Tables 1–4 for the four beams under two thermal load cases for $S = 5, 10, 20, 40$. The error in the FSDT and the TOT for $\bar{w}$ are large and almost the same, and there is only a marginal improvement or a marginal deterioration in the results for the existing ZIGT. The error in $\bar{w}$ for these theories, even for thin beams (a)–(d) with $S = 40$ are large, which for ZIGT are 50%, 100%, 2.6%, 100% for load case 1 and 3.1%, 6.6%, 1.2%, 23% for load case 2, respectively. The errors are the largest for the sandwich beam (d). The corresponding errors in $\bar{w}$ for the present HZIGT for $S = 40$ are generally one

Table 1
Exact results and % error of HZIGT, ZIGT, TOT and FSDT for beam (a)

S		Load case 1						Load case 2				
		Exact	HZIGT	ZIGT	TOT	FSDT		Exact	HZIGT	ZIGT	TOT	FSDT
5	$\bar{w}(-0.5h)$	−1.7810	−5.12	−89.8	−99.9	−101.0	$\bar{w}(0.5h)$	1.7115	−3.72	−66.5	−70.3	−70.5
10		−0.59040	−4.98	−87.5	−96.5	−97.7		0.82276	−2.03	−33.9	− 36.0	−36.2
20		−0.18334	−4.37	−76.8	−84.0	−85.0		0.60610	−0.70	−11.4	− 12.1	−12.2
40		−0.07130	−2.88	−50.5	−55.1	−55.8		0.55257	−0.19	−3.12	−3.32	−3.34
5	$\bar{\sigma}_x(-0.4h^+)$	1.0752	3.49	−42.4	−50.5	−50.7	$\bar{w}(-0.5h)$	1.0565	−7.10	−45.8	−51.9	−52.3
10		0.82612	0.52	−19.0	−21.9	−22.0		0.70246	−2.85	−22.6	−25.1	−25.2
20		0.73573	0.08	−5.86	−6.73	−6.75		0.58029	−0.89	−7.46	−8.23	−8.29
40		0.71049	0.02	−1.56	−1.78	−1.79		0.54642	−0.24	−2.03	−2.23	−2.25
5	$\bar{\sigma}_x(-0.5h)$	−0.93854	0.75	3.83	4.30	4.33	$\bar{\sigma}_x(0.5h)$	0.52042	10.8	−37.0	−39.3	−39.4
10		−0.96081	0.24	1.21	1.34	1.35		0.36673	2.68	−13.2	−14.0	−14.1
20		−0.96830	0.07	0.33	0.36	0.36		0.32650	0.66	−3.66	−3.91	−3.93
40		−0.97036	0.02	0.08	0.09	0.09		0.31640	0.16	−0.95	−1.01	−1.01
5	$\bar{\tau}_{zx}(0)$	−0.26318	−0.16	9.77	15.6	15.8	$\bar{\tau}_{zx}(-0.4h)$	−0.20319	0.96	0.98	1.16	1.17
10		−0.33492	0.13	3.07	4.36	4.39		−0.21710	0.24	0.31	0.36	0.36
20		−0.36166	0.05	0.82	1.12	1.13		−0.22216	0.06	0.09	0.09	0.09
40		−0.36919	0.01	0.21	0.28	0.28		−0.22357	0.01	0.02	0.03	0.03

Table 2
Exact results and % error of HZIGT, ZIGT, TOT and FSDT for beam (b)

S		Load case 1						Load case 2				
		Exact	HZIGT	ZIGT	TOT	FSDT		Exact	HZIGT	ZIGT	TOT	FSDT
5	$\bar{w}(0.5h)$	2.1524	−11.8	−100.0	−100.0	−100.0	$\bar{w}(0.5h)$	0.87019	−5.18	−91.4	−86.0	−79.8
10		0.56487	−12.7	−100.0	−100.0	−100.0		0.35729	−3.04	−57.1	−53.6	−49.6
20		0.14297	−12.9	−100.0	−100.0	−100.0		0.22551	−1.18	−22.8	−21.3	−19.8
40		0.03585	−12.9	−100.0	−100.0	−100.0		0.19227	−0.31	−6.64	−6.22	−5.76
5	$\bar{\sigma}_x(0.25h^-)$	−0.90214	0.30	−1.29	−1.29	−1.29	$\bar{w}(0)$	−0.18650	−16.3	−140.0	−165.0	−194.0
10		−0.93419	0.06	−0.34	−0.34	−0.34		0.08875	10.0	72.8	87.0	103.0
20		−0.94251	0.01	−0.08	−0.08	−0.08		0.15810	1.46	10.2	12.2	14.5
40		−0.94462	0.00	−0.02	−0.02	−0.02		0.17540	0.38	2.34	2.80	3.30
5	$\bar{\sigma}_x(0.5h)$	1.1752	6.13	−24.9	−24.9	−24.9	$\bar{\sigma}_x(0.5h)$	0.20642	4.11	−41.4	−36.9	−33.6
10		1.0086	1.51	−7.90	−7.90	−7.90		0.15867	1.15	−14.2	−12.6	−11.5
20		0.96152	0.38	−2.12	−2.12	−2.12		0.14589	0.31	−3.89	−3.45	−3.15
40		0.94939	0.09	−0.54	−0.54	−0.54		0.14260	0.12	−0.95	−0.84	−0.76
5	$\bar{\tau}_{zx}(0.25h)$	0.69183	2.75	0.24	0.24	0.24	$\bar{\tau}_{zx}(0)$	−0.11109	2.21	−4.38	−3.44	−2.95
10		0.72932	0.67	0.05	0.05	0.05		−0.11124	0.52	−1.19	−0.93	−0.82
20		0.73914	0.17	0.01	0.01	0.01		−0.11122	0.12	−0.31	−0.25	−0.22
40		0.74162	0.04	0.00	0.00	0.00		−0.11124	0.00	−0.11	−0.10	−0.09

Table 3
Exact results and % error of HZIGT, ZIGT, TOT and FSDT for beam (c)

S		Load case 1						Load case 2				
		Exact	HZIGT	ZIGT	TOT	FSDT		Exact	HZIGT	ZIGT	TOT	FSDT
5	$\bar{w}(-0.5h)$	−4.9319	−11.0	−57.0	−61.3	−64.4	$\bar{w}(-0.5h)$	2.9142	−12.6	−40.1	−47.3	−48.5
10		−2.6469	−5.79	−28.3	−30.4	−31.9		1.8747	−5.24	−16.1	−19.9	−19.4
20		−2.0291	−1.95	−9.39	−10.1	−10.6		1.6047	−1.55	−4.73	−5.58	−5.71
40		−1.8714	−0.53	−2.55	−2.74	−2.87		1.5364	−0.40	−1.22	−1.44	−1.48
5	$\bar{w}(0.5h)$	−0.64725	−2.12	228.0	195.0	172.0	$\bar{w}(0.5h)$	2.7645	−8.10	−36.8	−44.4	−45.7
10		−1.5237	−0.92	24.53	20.9	18.3		1.8416	−3.56	−14.6	−17.5	−18.0
20		−1.7448	−0.25	5.38	4.57	4.00		1.5967	−1.06	−4.25	−5.10	−5.24
40		−1.8001	−0.06	1.31	1.11	0.97		1.5344	−0.27	−1.09	−1.32	−1.36
5	$\bar{\sigma}_x(-0.25h^+)$	2.2792	−3.39	−11.3	−12.8	−12.6	$\bar{\sigma}_x(-0.25h^+)$	−1.2588	−7.59	−5.78	−7.40	−7.32
10		2.1417	−1.19	−3.42	−3.82	−3.77		−1.1978	−2.19	−1.71	−2.15	−2.13
20		2.1002	−0.32	−0.90	−1.00	−0.99		−1.1803	−0.57	−0.45	−0.56	−0.55
40		2.0893	−0.08	−0.22	−0.25	−0.25		−1.1757	−0.14	−0.11	−0.14	−0.14
5	$\bar{\sigma}_x(0.25h^-)$	−0.90585	0.47	−0.56	−0.30	−0.23	$\bar{\sigma}_x(0.5h)$	0.87469	3.13	−8.93	−12.3	−12.9
10		−0.95311	0.13	−0.13	−0.07	−0.05		0.79977	0.64	−2.73	−3.69	−3.84
20		−0.96584	0.03	−0.03	−0.02	−0.01		0.77866	0.15	−0.72	−0.97	−1.00
40		−0.96908	0.01	0.00	0.00	0.00		0.77314	0.05	−0.17	−0.23	−0.24
5	$\bar{\tau}_{zx}(-0.25h)$	0.59648	4.51	8.57	8.98	9.03	$\bar{\tau}_{zx}(-0.25h)$	−0.48938	4.92	5.25	5.62	5.63
10		0.65290	1.18	2.15	2.25	2.26		−0.51310	1.25	1.33	1.41	1.42
20		0.66851	0.30	0.54	0.56	0.56		−0.51941	0.31	0.33	0.35	0.36
40		0.67252	0.07	0.13	0.14	0.14		−0.52102	0.08	0.08	0.09	0.09

order less, being 2.9%, 13%, 0.53%, 1.5% and 0.19%, 0.31%, 0.40%, 0.13% for load cases 1 and 2, respectively, with the largest error for the symmetric composite beam (b) for load case 1. Even for the

Table 4
Exact results and % error of HZIGT, ZIGT, TOT and FSDT for beam (d)

S		Load case 1						Load case 2				
		Exact	HZIGT	ZIGT	TOT	FSDT		Exact	HZIGT	ZIGT	TOT	FSDT
5	$\bar{w}(0.5h)$	2.3206	0.13	−100.0	−100.0	−100.0	$10\bar{w}(0)$	−1.7136	1.18	−110.0	−110.0	−109.0
10		0.62669	0.03	−100.0	−100.0	−100.0		−0.30710	1.14	−153.0	−152.0	−152.0
20		0.15906	0.53	−100.0	−100.0	−100.0		0.04304	−1.65	272.0	272.0	271.0
40		0.04081	−1.54	−100.0	−100.0	−100.0		0.13020	0.13	22.7	22.7	22.6
5	$10\bar{\sigma}_x(0.5h)$	2.0233	0.83	−100.0	−100.0	−100.0	$10\bar{w}(0.5h)$	5.3312	−0.27	−96.9	−96.9	−97.0
10		0.55426	−0.36	−100.0	−100.0	−100.0		1.4742	−0.22	−89.1	−89.1	−89.2
20		0.14314	−0.64	−99.2	−99.2	−99.2		0.48962	−0.14	−67.3	−67.3	−67.4
40		0.03730	−0.69	−95.8	−95.8	−95.8		0.24192	0.07	−33.9	−34.0	−34.0
5	$10^2\bar{\tau}_{zx}(0.45h)$	1.5387	0.86	−100.0	−100.0	−100.0	$10^2\bar{\sigma}_x(0.5h)$	3.2254	5.36	−113.0	−113.0	−113.0
10		0.42422	−0.65	−99.8	−99.8	−99.8		0.52979	6.81	−176.0	−176.0	−176.0
20		0.11071	−1.00	−98.0	−98.0	−98.0		−0.16868	−5.53	154.0	139.0	139.0
40		0.02989	−1.02	−91.3	−91.3	−91.3		−0.34717	−1.56	22.9	16.0	16.0
5							$10^3\bar{\tau}_{zx}(0.45h)$	2.0693	8.20	−115.0	−115.0	−115.0
10								0.31029	11.5	−198.0	−198.0	−198.0
20								−0.14128	−1.31	114.0	114.0	114.0
40								−0.26863	−2.62	12.6	12.6	12.6

moderately thick beam with $S = 10$, the maximum error in $\bar{w}$ for the present HZIGT is 5.8%, except the symmetric composite beam (b) for load 1 with an error of 13%, whereas the error for the other theories ranges from 16% to 152% with the largest error for the sandwich beam. For beam (b) under load 1, HZIGT reproduces the $\bar{w}$ profile very well with no error in the central deflection and a maximum error of 13% on the faces.

A similar comparison of the results for the stresses reveals that the TOT results are close to the FSDT results and the existing ZIGT results are only marginally better or marginally worse than the TOT results. However, the errors in the stresses for the present HZIGT are relatively smaller, even one order less in some cases, except for the maximum compressive normal stress in beam (c) under thermal load case 2 and for the shear stress for beam (b) for thermal load 1 wherein there is an increase. However, the errors themselves for these exceptional cases are small. Moreover, in beam (c) under load case 2, the error in the maximum tensile normal stress has reduced to 3.13% in HZIGT from 8.93% in ZIGT. The FSDT, TOT and existing ZIGT yield highly erroneous stress results even for thin sandwich beams (d) with $S = 40$. The error in the stresses predicted by the existing ZIGT and the present HZIGT for thin beams (a)–(c) with $S = 40$ is quite small with the error of the HZIGT being generally smaller. For the moderately thick beams (a)–(c) with $S = 10$, the present HZIGT yields much accurate stresses than the existing ZIGT with errors almost one order less, except for the anti-symmetric beam (c) for load case 2 for which the errors in the maximum compressive stress are 2.19% and 1.71%, respectively. The errors in the stresses of existing ZIGT, TOT and FSDT, for the load case 2 for these moderately thick beams with $S = 10$, are quite large varying from 1.71% to 23% for the ZIGT, whereas the maximum error of the present HZIGT is only 2.2%.

5. Conclusions

An efficient new zigzag theory is presented, based on zigzag third order variation of the in-plane displacement and sub-layerwise quadratic variation of the transverse displacement accounting explicitly for the thermal contribution to the transverse normal strain. The shear traction-free conditions at the top and

the bottom of the beam and the shear continuity conditions at the layer interfaces are satisfied exactly to reduce the primary displacement variables to three. The thermal field is approximated to be sub-layerwise linear across the thickness. The new HOT HZIGT is assessed by comparison with the exact 2D thermo-elasticity solution of simply-supported beams for longitudinally sinusoidal temperature distribution with equal temperature rise of the top and bottom surfaces of the beam and with equal rise and fall of temperature of these surfaces. The temperature profiles across the thickness are based on the heat conduction equation. A benchmark test beam, symmetric and anti-symmetric composite beams and sandwich beams are analysed to cover a wide range of temperature profiles across the thickness. It is concluded from the comparative study that the TOT and the FSDT results are almost the same and the existing ZIGT results are only marginally better (in some cases marginally worse) than those of the TOT and the FSDT. The errors are particularly large for the sandwich beams. These theories should not be used for moderately thick beams with $S = 10$ and even for some thin beams with $S = 40$ in which the errors are significant. The present HZIGT yields much more accurate results for the deflection and the stresses with few exceptions for which the errors themselves are not large. The present HZIGT can be used for all types of beams and thermal loadings with small error for $S \geqslant 10$ and even for some thick beams with $S = 5$. The new theory generally reproduces quite well the thickness distributions of the stresses and the transverse displacement with small error. The new theory developed herein is much more accurate and yet as efficient as the existing ZIGT, TOT and FSDT, since it is formulated in terms of only three primary displacements.

Acknowledgements

The authors are grateful to reviewers whose constructive suggestions have been incorporated to improve the paper.

References

Aitharaju, V.R., Averill, R.C., 1999. C^0 zigzag finite element for analysis of laminated composite beams. J. Eng. Mech. 125, 323–330.

Ali, J.S.M., Bhaskar, K., Varadan, T.K., 1999. A new theory for accurate thermal/mechanical flexural analysis of symmetric laminated plates. Compos. Struct. 45, 227–232.

Averill, R.C., Yip, Y.C., 1996. An efficient thick beam theory and finite element model with zigzag/sub-laminate approximations. Am. Inst. Aeronaut. Astronaut. J. 34, 1626–1632.

Bhaskar, K., Vardan, T.K., Ali, J.S.M., 1996. Thermo-elastic solution for orthotropic and anisotropic composite laminates. Composites Part B 27B, 415–420.

Bickford, W.B., 1982. A Consistent higher-order beam theory. Dev. Th. Appl. Mech. 11, 137–142.

Carrera, E., 2001. Developments, ideas and evaluations based upon the Reissner's mixed variational theorem in the modelling of multilayered plates and shells. Appl. Mech. Rev. 54, 301–329.

Carrera, E., 2002. Temperature profile influence on layered plates response considering classical and advanced theories. Am. Inst. Aeronaut. Astronaut. J. 40, 1885–1896.

Cho, M., Parmerter, R.R., 1993. Efficient higher order composite plate theory for general lamination configurations. Am. Inst. Aeronaut. Astronaut. J. 31, 1299–1306.

Di Sciuva, M., 1986. Bending, vibration and buckling of simply-supported thick multilayered orthotropic plates: an evaluation of a new displacement model. J. Sound Vib. 105, 425–442.

Heyliger, P.R., Reddy, J.N., 1988. A higher-order beam finite element for bending and vibration problems. J. Sound Vib. 126, 309–326.

Icardi, U., 2001. A three dimensional zigzag theory for analysis of thick laminated beams. Compos. Struct. 52, 123–135.

Kant, T., Manjunath, B.S., 1989. Refined theories for composite and sandwich beams with C^0 finite elements. Comput. Struct. 33, 755–764.

Kant, T., Manjunath, B.S., 1990. Higher-order theories for symmetric and unsymmetric fibre reinforced composite beams with C^0 finite elements. Finite Elem. Anal. Des. 6, 303–320.

Li, X., Liu, D., 1995. Zigzag theory for composite laminates. AIAA J. 33, 1163–1165.

Liu, S., Soldatos, K.P., 2002. On the prediction improvement of transverse stress distribution in cross-ply laminated beams: advanced versus conventional beam modelling. Int. J. Mech. Sci. 44, 287–304.

Marur, S.R., Kant, T., 1997. On the performance of higher order theories for transient dynamic analysis of sandwich and composite beams. Comput. Struct. 65, 741–759.

Noor, A.K., Burton, W.S., 1994. Three-dimensional solutions for initially stressed structural sandwiches. J. Eng. Mech. ASCE 120, 284–303.

Noor, A.K., Malik, M., 2000. An assessment of modelling approaches for thermo-mechanical stress analysis of laminated composite panels. Comput. Mech. 25, 43–58.

Park, J.W., Kim, Y.H., 2002. Re-analysis procedure for laminated plates using FSDT finite element method. Comput. Mech. 29, 226–242.

Rao, D.K., 1978. Frequencies and loss factors of multilayered sandwich beams. J. Machine Des. 100, 667–674.

Reddy, J.N., 1984. A simple higher-order theory for laminated composite plates. J. Appl. Mech. 51, 745–752.

Reddy, J.N., 1997. Mechanics of Laminated Composite Plates—Theory and Analysis. CRC Press, Boca Raton, FL.

Savoia, M., Laudiero, F., Tralli, A., 1993. A refined theory for laminated beams: part I—a new higher order approach. Meccanica 28, 39–51.

Shu, X., Soldatos, K.P., 2000. Cylindrical bending of angle-ply laminates subjected to different sets of edge boundary conditions. Int. J. Solids Struct. 37, 4289–4307.

Soldatos, K.P., Elishakoff, I., 1992. A transverse shear and normal deformable orthotropic beam theory. J. Sound Vib. 154, 528–533.

Soldatos, K.P., Liu, S.L., 2001. On the generalised plane strain deformations of thick anisotropic composite laminated plates. Int. J. Solids Struct. 38, 479–482.

Soldatos, K.P., Liu, S.L., 2003. On accurate prediction of stress distributions in laminates subjected to thermomechanical loading. In: Proc. 5th Cong. on Thermal Stresses and Related Topics, Virginia Tech Institute and State University Blacksburg, VA, June 8–11, 2003, pp. TA.4.5.1–TA.4.5.4.

Soldatos, K.P., Watson, P., 1997. A general theory for the accurate stress analysis of homogeneous and laminated composite beams. Int. J. Solids Struct. 22, 2857–2885.

Tanigawa, Y., Murakami, H., Ootao, Y., 1989. Transient thermal stress analysis of a laminated composite beam. J. Thermal Stresses 12, 25–39.

Xioping, S., Liangxin, S., 1994. Thermo-mechanical buckling of laminated composite plates with higher order transverse shear deformation. Comput. Struct. 53, 1–7.

Xu, K., Noor, A.K., Tang, Y.Y., 1995. Three-dimensional solutions for coupled thermo-electro-elastic response of multilayered plates. Comput. Meth. Appl. Mech. Eng. 126, 355–371.